Lawrence Berkeley National Laboratory
Recent Work

Title

Amazon forest response to CO2 fertilization dependent on plant phosphorus acquisition

Authors

Fleischer, K
Rammig, A
De Kauwe, MG
et al.

Peer reviewed

Amazon forest response to CO₂ fertilization dependent on plant phosphorus acquisition

Katrin Fleischer[1]*, Anja Rammig[1], Martin G. De Kauwe[2,3], Anthony P. Walker[4], Tomas F. Domingues[5], Lucia Fuchslueger[6,7], Sabrina Garcia[6], Daniel S. Goll[8,9], Adriana Grandis[10], Mingkai Jiang[11], Vanessa Haverd[12], Florian Hofhansl[13], Jennifer A. Holm[14], Bart Kruijt[15], Felix Leung[16,17], Belinda E. Medlyn[11], Lina M. Mercado[16,18], Richard J. Norby[4], Bernard Pak[19], Celso von Randow[20], Carlos A. Quesada[6], Karst J. Schaap[6], Oscar J. Valverde-Barrantes[21], Ying-Ping Wang[19], Xiaojuan Yang[4], Sönke Zaehle[22], Qing Zhu[14] and David M. Lapola[23]

[1] Land Surface–Atmosphere Interactions, Technical University of Munich, Munich, Germany. [2] Climate Change Research Centre, University of New South Wales, Sydney, New South Wales, Australia. [3] ARC Centre of Excellence for Climate Extremes, Sydney, New South Wales, Australia. [4]Environmental Sciences Division and Climate Change Science Institute, Oak Ridge National Laboratory, Oak Ridge, TN, USA. [5] FFCLRP, Department of Biology, University of São Paulo, Ribeirão Preto, Brazil. [6]National Institute of Amazonian Research (INPA), Manaus, Brazil. [7] Department of Biology, University of Antwerp, Antwerp, Belgium. [8]Laboratoire des Sciences du Climat et de l'Environnement, LSCE/IPSL, CEA–CNRS–UVSQ, Saint-Aubin, France. [9]Lehrstuhl für Physische Geographie mit Schwerpunkt Klimaforschung, Universität Augsburg, Augsburg, Germany. [10]Department of Botany, University of São Paulo, São Paulo, Brazil. [11]Hawkesbury Institute for the Environment, Western Sydney University, Sydney, New South Wales, Australia. [12]CSIRO Oceans and Atmosphere, Canberra, Australian Capital Territory, Australia. [13]International Institute for Applied Systems Analysis, Laxenburg, Austria. [14]Lawrence Berkeley National Laboratory, Berkeley, CA, USA. [15]Alterra Wageningen, Wageningen, The Netherlands. [16]College of Life and Environmental Sciences, University of Exeter, Exeter, UK. [17]Institute of Environment, Energy and Sustainability, The Chinese University of Hong Kong, Hong Kong, Hong Kong. [18]Centre for Ecology and Hydrology, Wallingford, UK. [19]CSIRO Oceans and Atmosphere, Aspendale, Victoria, Australia. [20]National Institute for Space Research (INPE), São José dos Campos, Brazil. [21]International Center of Tropical Botany, Florida International University, Miami, FL, USA. [22]Max-Planck Institute for Biogeochemistry, Jena, Germany. [23]Center for Meteorological and Climatic Research Applied to Agriculture, University of Campinas, Campinas, Brazil. *e-mail: katrin.fleischer@tum.de

Abstract

Global terrestrial models currently predict that the Amazon rainforest will continue to act as a carbon sink in the future, primarily owing to the rising atmospheric carbon dioxide (CO₂) concentration. Soil phosphorus impoverishment in parts of the Amazon basin largely controls its functioning, but the role of phosphorus availability has not been considered in global model ensembles—for example, during the Fifth Climate Model

Intercomparison Project. Here we simulate the planned free-air CO_2 enrichment experiment AmazonFACE with an ensemble of 14 terrestrial ecosystem models. We show that phosphorus availability reduces the projected CO_2-induced biomass carbon growth by about 50% to 79 ± 63 g C m^{-2} yr^{-1} over 15 years compared to estimates from carbon and carbon–nitrogen models. Our results suggest that the resilience of the region to climate change may be much less than previously assumed. Variation in the biomass carbon response among the phosphorus-enabled models is considerable, ranging from 5 to 140 g C m^{-2} yr^{-1}, owing to the contrasting plant phosphorus use and acquisition strategies considered among the models. The Amazon forest response thus depends on the interactions and relative contributions of the phosphorus acquisition and use strategies across individuals, and to what extent these processes can be upregulated under elevated CO_2.

Introduction

The intact Amazon rainforest acts as a substantial carbon (C) sink that completely offsets the carbon dioxide (CO_2) emissions from fossil fuel combustion and land use change in the Amazon region[1,2]. Increasing atmospheric CO_2 concentrations from anthropogenic activity may be the primary factor for the current Amazon net C sink[1,3], via so-called CO_2 fertilization (an increase in photosynthetic C uptake by plants under a higher CO_2), which is projected to continue into the future by global models[4,5,6]. The CO_2 fertilization effect has been observed in field experiments that were conducted predominantly in the temperate zone. In these experiments, the elevated carbon dioxide (eCO_2)-induced increase in C uptake was generally low when other factors, such as soil nitrogen (N), were limiting[7,8,9]. So far, whole-ecosystem-scale experiments, that is, free-air CO_2 enrichment (FACE) experiments, have not been conducted in the tropics[10,11].

Over large parts of the Amazon and the tropics worldwide, phosphorus (P), not N, is assumed to be the key limiting nutrient, as most P has been lost or occluded from plant uptake during millions of years of soil pedogenesis[12,13]. Forests that grow on these highly weathered old soils may nonetheless be highly productive due to the evolution of multiple strategies for P acquisition and use, which enable a tight cycling of P between plants, microorganisms and soils[14,15]. Despite this knowledge, to quantify the control of P on plant physiology, growth and plant–soil–microbial interactions in global models, and hence its role in the forests' responses to eCO_2, remains a challenge[16,17]. This challenge is exacerbated by the scarcity of observations and distinctive plant species responses in hyperdiverse tropical forests[18].

Predicted nutrient feedbacks to eCO_2 for AmazonFACE

Here we study the potential interactions between eCO_2 and nutrient (N and P) feedbacks in a mature Amazonian rainforest by simulating the planned AmazonFACE experiment (+200 ppm; https://amazonface.inpa.gov.br/) with

an ensemble of ecosystem models ($n = 14$ (the model details are given in Supplementary Table 3)), which includes three C, five carbon–nitrogen (CN) and six carbon–nitrogen–phosphorus (CNP) models[19,20,21,22,23,24]. The AmazonFACE experiment is located in a well-studied, highly productive tropical forest in Central Amazonia[25,26], which grows on a strongly weathered terra firme ferralsol. This ecosystem represents the low end of the plant-available P spectrum in the Amazon, consistent with ~32% of the Amazon rainforest's cover fraction[27]. In situ measurements were used to parameterize the models and to evaluate simulated ambient conditions (Supplementary Tables 1 and 2). Our aim was to generate a priori model-based hypotheses to highlight the current state of knowledge and guide measurement strategies for AmazonFACE and other ecosystem manipulation experiments to gain crucial process understanding of P control on the CO_2 fertilization effect.

Simulated eCO_2 (+200 ppm) had a positive effect on plant biomass C across all the models, but was weakest in the CNP models (Fig. 1a). The eCO_2 conditions induced average biomass C gains of 163 ± 65, 145 ± 83 and 79 ± 63 g C m^{-2} yr^{-1} (mean ± s.d.) over 15 years in the C, CN and CNP models, respectively (Fig. 1a). Limitations by P thus reduced the predicted biomass C sink by 52 and 46% compared to that in the C and CN models, respectively, with considerable variation across and within model groups (Supplementary Fig. 1). Plot inventories at the AmazonFACE site during the 2000s indicate an above-ground biomass increment of 23 g C m^2 yr^{-1}, substantially below the Amazon-wide[1] estimate of 64 g C m^2 yr^{-1}. The model ensemble represents ambient conditions, such as productivity and leaf area index, reasonably well, but ensemble members show divergence in other ecosystem characteristics, such as the biomass C increment, which range from 5 to 114 g C m^2 yr^{-1}. There is, however, no clear pattern in performance between the model groups, so that we judge that these differences do not have a bearing on the conclusions of our study (further discussion in Supplementary Fig. 2).
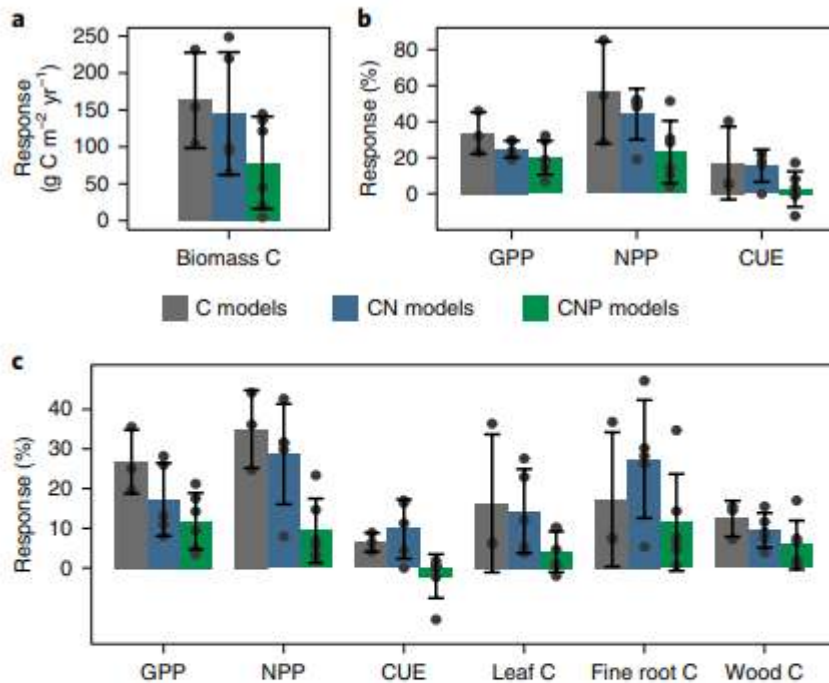
Fig. 1 | The predicted effect of eCO$_2$ on biomass C, productivity and biomass compartments for C, CN and CNP models. a, The final response of biomass growth, calculated as the mean annual response over 15 years of eCO$_2$. **b**, The first-year response of productivity (GPP and NPP) and CUE. **c**, The 15-year response of productivity, CUE and leaf, fine root and wood C (calculated as the mean response of the 13th to 17th years). Responses to eCO$_2$ are the differences between the elevated and ambient model run, shown as mean and s.d. (black lines) per model group, with individual model results as dots.

Differing model responses to P limitation

Gross and net primary productivity (GPP and NPP, respectively) are both stimulated by eCO$_2$ in all models, both initially (after one year of eCO$_2$) and until the end of the simulation. The CNP models show the strongest decline from the initial response due to P limitation (Fig. 1b,c). The final response of NPP to eCO$_2$ was a 35%, 29% and 9% stimulation for the C, CN and CNP models, respectively. In general, in the CN and CNP models, nutrient limitation is defined as the nutrient demand being greater than the nutrient supply. However, the models differ in their assumptions on how nutrient limitation controls productivity and C allocation in response to eCO$_2$, so that divergent responses on plant C use efficiency (CUE = NPP/GPP) are simulated (Supplementary Table 3). In some CN models, CUE increases because the N limitation is hypothesized to reduce autotrophic respiration via a lower tissue N content. Some CNP models, however, assume a direct downregulation of growth and hence the plant CUE decreases (Supplementary Fig. 3). Elevated CO$_2$ induced higher fine root investments of NPP in some CN and CNP models to aid nutrient acquisition (Fig. 1c and Supplementary Fig. 4). The predicted

changes in allocation with eCO_2 cause a general increase in biomass turnover across all but one of the models, and partially offset the positive biomass response (Supplementary Table 4). Changes in turnover play a minor role in our 15 year simulation period, but rather control the long-term future CO_2 effect on the biomass C sink[28,29].

Plant growth under eCO_2 is lowest in the CNP models as the low availability of soil labile P restricts P uptake either immediately or over time (Supplementary Fig. 5). We considered the modelled P limitation on plant growth to be realistic, as the models and observations agree that soil labile P is very low (Supplementary Fig. 2). Other site observations support the fact that P is extremely critical for plant productivity, such as high leaf N:P ratios of 37 and a high plant P resorption (before litter fall) of 78% (Supplementary Table 1). Although P limitation consistently reduces the eCO_2-induced biomass C sink, there is significant variation among CNP models due to contrasting process representations (Fig. 2 and Supplementary Table 3). P shortages downregulate growth (that is, NPP) in all the CNP models, directly or via photosynthesis. The major differences in the model assumptions relate to how they modify P supply and demand to alleviate plant P shortages, which include either (1) enhancing the plant P use efficiency (PUE = NPP/P uptake) or (2) upregulating the P acquisition mechanisms. The models assume that PUE may change if the tissue nutrient ratios are flexible, if the C allocation changes among tissues with different stoichiometry and/or if P resorption is variable (Fig. 2). Flexible stoichiometry is considered in all the CNP models except ELM-CTC, although with varying degrees of flexibility. A greater fine root C allocation with plant P stress is considered in some, and P resorption is a fixed fraction of leaf tissue P in all the models (Fig. 2).
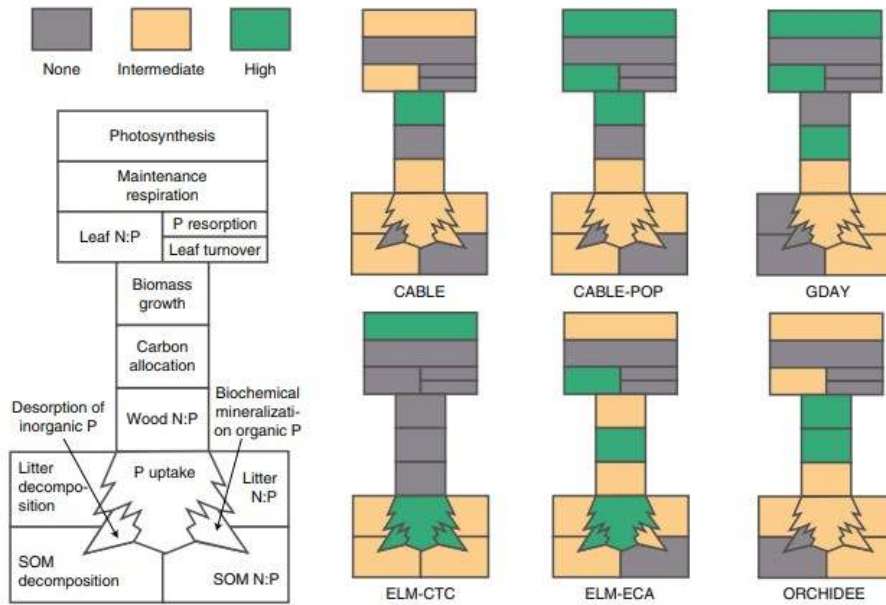
Fig. 2 | Strength of P feedbacks in controlling the biomass C response to eCO₂ for the six CNP models. The degree to which the modelled P feedback on ecosystem processes controls the response of biomass C to eCO₂ in our simulations (none, intermediate and high). P limitation downregulates photosynthesis or growth under eCO₂ in all the models. Maintenance respiration, leaf turnover and P resorption are not controlled by the P cycle in any of the models. The leaf N:P ratio responds to eCO₂ in most of the models. The desorption of P from mineral surfaces is considered only in ELM-ECA and ELM-CTC, and biochemical P mineralization is considered in many of the models, but effectively responsive only in ELM-CTC (Supplementary Table 3). SOM, soil organic matter.

The CNP models differ in their representation of soil P acquisition mechanisms; three of the six models (ELM-ECA, ELM-CTC and GDAY) consider the desorption of P from mineral surfaces (that is, the secondary or strongly sorbed P pool), whereas the others assume P in these pools to be unavailable to plants. All the models include the biochemical mineralization of organic P via phosphatase, but only three (ELM-ECA, ELM-CTC and ORCHIDEE) include the functionality to increase the P acquisition via this mechanism under plant P stress (Fig. 2 and Supplementary Table 3). Litter and soil stoichiometry are considered with varying degrees of flexibility. Soil labile P limits the microbial decomposition rates of litter and soil, so that decomposition is reduced when immobilization demands for P exceed the soil labile P availability (Fig. 2 and Supplementary Table 3).

Enhanced PUE and acquisition due to eCO₂

Diverging representations of plant P use and acquisition among the CNP models cause predictions of the eCO₂-induced biomass C sink to range from $5 \, \mathrm{g \, C \, m^{-2} \, yr^{-1}}$ to $140 \, \mathrm{g \, C \, m^{-2} \, yr^{-1}}$ (Fig. 3a and Supplementary Fig. 1). Greater plant PUE occurred in four of the models, for which shifts in tissue C:N and N:P ratios due to eCO₂ led to increases in biomass C:P that ranged from ~200 to $1,600 \, \mathrm{g \, C \, g \, P^{-1}}$ (Fig. 3c). A higher fine root investment with eCO₂, at the expense of less 'P-costly' wood, offset some increases in PUE in some models (Fig. 3b). A flexible biomass stoichiometry altered the decomposition dynamics and induced progressive P limitation in response to eCO₂, that is, the litter stoichiometry shifted towards a lower quality (less N and P in

relation to C), which reduces the net P mineralization rates from microbial decomposition and so causes P to become increasingly unavailable to plants and accumulating in soil organic matter (Fig. 3d,e). This plant–soil–microbial feedback slowed the cycling of P in the ecosystem and exacerbated the initial P limitation (Vitousek[30] reports a similar feedback during pedogenesis).
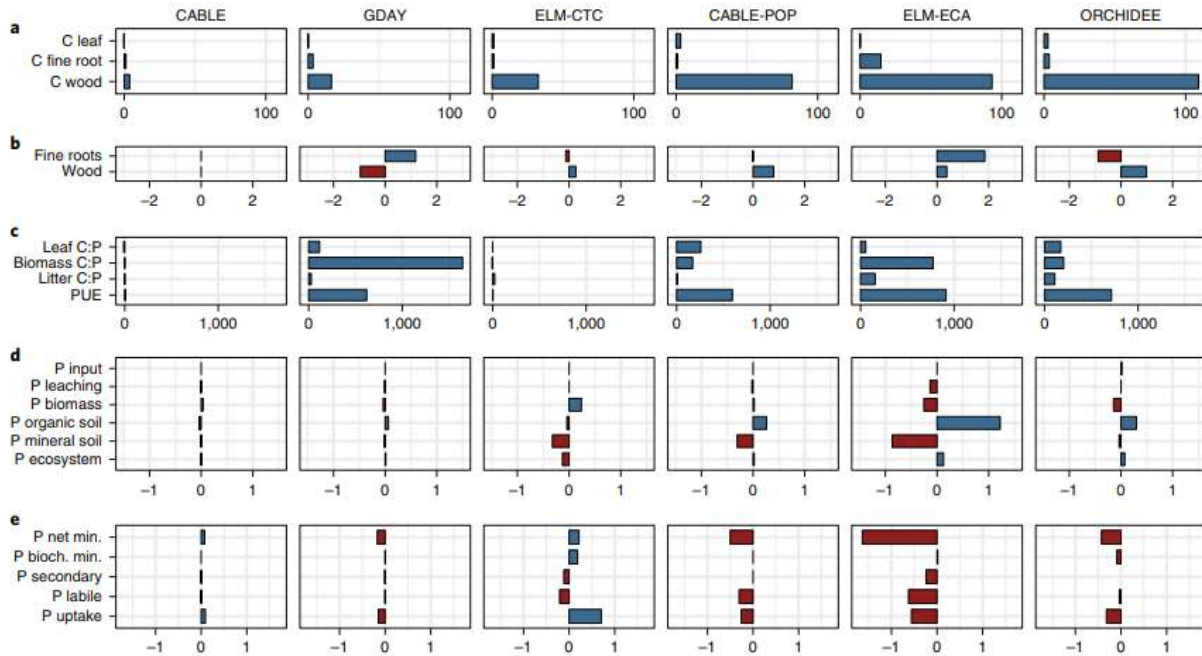
Fig. 3 | Key responses of biomass C gain, stoichiometry, allocation and P dynamics to eCO₂ for the CNP models. Blue denotes a positive response; red denotes a negative response. **a**, Mean annual change in standing leaf, fine root and wood C over 15 years (g C m⁻² yr⁻¹), which increases across the models from left to right (CABLE, GDAY, ELM-CTC, CABLE-POP, ELM-ECA, and ORCHIDEE). **b**, The mean change in C allocation for fine roots and wood (%). **c**, Mean change in tissue stoichiometry in absolute terms (g C g P⁻¹) and change in PUE over 15 years (g C g P⁻¹ yr⁻¹). **d**, The P ecosystem retention in terms of the mean change in the ecosystem P input and output (leaching) fluxes (g P m⁻² yr⁻¹) and in the final P stock in the biomass, organic soil, mineral soil and total ecosystem (g P m⁻²). **e**, Mean change in plant P acquisition processes, namely net P mineralization (min), biochemical (bioch) P mineralization, and P uptake (g P m⁻² yr⁻¹), and in the secondary and labile P pools (g P m⁻²). For both **d** and **e**, the P flux changes are differences in the cumulative fluxes after 15 years and the P pool changes are differences in pools after 15 years.

Enhanced plant P acquisition under eCO₂ effectively alleviated the plant P limitation in two CNP models (ELM-CTC and ELM-ECA) (Fig. 3e). In both, eCO₂ increased the liberation of P from the secondary pool, as a higher plant P demand and uptake diminished the labile P pool, which in turn caused higher desorption rates. P desorption is thus only indirectly, and not mechanistically, enhanced by plants in these models. Biochemical mineralization of organic P under eCO₂ responded positively in both of the models, but added only notably to additional P acquisition in ELM-CTC (Fig. 3e). Although three of the CNP models simulated higher fine root investments, the actual P uptake return per fine root increment was marginal or came only into effect in the long term (Supplementary Fig. 6).

Observations document ample N cycling in the system, for example, high leaf N contents, indicative δ¹⁵N values, high rates of N oxide emissions and low leaf N resorption[31,32], and thereby suggest that plant growth is not directly affected by N availability. The CN models, however, simulate an

increased N use efficiency and biomass C:N ratios in response to insufficient N uptake under eCO_2 (Supplementary Fig. 5). Plant N availability may be underestimated in the models because the plant-available mineral N supply was <7 g N m^{-2} across all the models, as opposed to 17.5 g N m^{-2} observed in the top 10 cm alone (Supplementary Fig. 2). These results highlight an important gap in our knowledge that relates to the dynamics of tropical N cycling and its potential interaction with P dynamics (Table 1).

Table 1 | Key processes and variables requiring observational estimates to reduce uncertainty in P cycle control on eCO_2 effects in ecosystem models

Process	Measurements needed
H1, Plant C budget	
Canopy scale C assimilation	Seasonal dynamics of leaf area and photosynthetic capacity Photosynthetic acclimation
Plant tissue respiration	Control of drought stress, nutrient limitation and P content Wood and root respiration
Biomass growth	Below-ground biomass compartments Long-term growth rates
H2, Plant P use	
Plant tissue C:P and N:P stoichiometry	Plasticity versus adaptation to environmental change Functionality of tissue P Wood P content and stoichiometry
Plant tissue P resorption	P content in live tissue and/or fresh litter (resorption effiency and/or proficiency) Plasticity versus adaptation to environmental change
H3, Plant P acquisition	
P desorption due to plant exudation	Flux and interactions with microorganisms Cost of exudation versus P return for plant
P acquisition due to fine root production	Surface litter fine root dynamics Fine root allocation fractions Fine root productivity vs. plant P uptake
Biochemical P mineralization (via phosphatase)	Phosphatase activity and relation to P mineralization Plant production of phosphatase vs. plant-induced production by microorganisms Cost of phosphatase production vs. plant P acquisition
Other interactions	
Plant N availability	Ecosystem N budget Symbiotic and free-living N fixation Control of N availability on P acquisition and other N:P interactions
Plant water availability	Control on P mineralization and transport dynamics Interacting control of water and P limitation on the eCO_2 effect

Model-based hypotheses for the AmazonFACE experiment

In summary, the model ensemble encapsulates a range of plausible hypotheses and represents a potential range of biomass C responses to

eCO$_2$ under a low soil P availability. The assumption of a lacking ability of plants to acquire more soil P and a limited capacity for plants to use P more efficiently resulted in an effectively zero biomass C gain with eCO$_2$. Conversely, flexible stoichiometry, in combination with an enhanced plant P acquisition, were the key mechanistic responses that led to biomass C gain with eCO$_2$. Divergences in the simulated eCO$_2$ response lead us to the following testable hypotheses, and call for directed field measurements (Table 1):

H1: low soil P availability will strongly constrain the future plant biomass growth response to eCO$_2$ either by downregulating photosynthesis or limiting plant growth directly, or a combination thereof.

H2: despite the limited soil P supply, plasticity in vegetation stoichiometry and allocation patterns will allow for some biomass growth under eCO$_2$.

H3: plants will increase investments in P acquisition to increase P supply and allow biomass growth under eCO$_2$ either via a greater P interception through fine root production or via a greater P liberation from P desorption or the biochemical mineralization of organic P.

These model-based hypotheses deepen a previous analysis of potential N and P limitation on terrestrial C accumulation based on mass balance principle[33]. Furthermore, we add to a model intercomparison carried out in advance of the EucFACE experiment[34] by extending the range of plant P feedbacks considered across CNP models. This work highlights H1: two stoichiometrically constrained CNP models predicted that a strong P limitation will curtail the growth response to eCO$_2$ in Australia. Consistent with this hypothesis, above-ground growth has not increased with eCO$_2$ in that experiment over the initial years[35]. This finding underlines that monitoring efforts need to place a strong(er) focus on below-ground C and nutrient dynamics, in addition to canopy-scale photosynthesis and above-ground growth dynamics. Additionally, the autotrophic respiration dependence on P content and plant stress from drought or nutrient limitation needs further monitoring during experiments to fully elucidate the plant C budget and address H1 (Table 1).

Nutrient fertilization experiments support H2, as plasticity in leaf stoichiometry at the individual level, along with plasticity in P resorption, was observed[36]. Across the Amazon, community-weighted leaf N:P ratios in the field varied from 13 to 42 g N g P^{-1} ($n = 64$)[32], which place our site, with a mean of 37, closer to the high end. GDAY predicted the most plausible increase in the leaf N:P ratio from 34 to 38 (Supplementary Fig. 7). Two models predicted strong increases in the leaf N:P ratio with eCO$_2$, but began with much lower initial values. The degree to which plasticity in stoichiometry and resorption can aid plant PUE under eCO$_2$ in highly P-limited sites that are already at the end of the observed spectrum remains to be seen (H2). Monitoring plant-tissue stoichiometry, which includes wood with much higher N:P ratios, combined with assessments of the P resorption in

CO_2 and nutrient fertilization experiments, will reduce the uncertainties (Table 1).

Based on previous observations[8], a number of models assume an increased fine root investment, as well as higher biochemical P mineralization and P desorption from mineral surfaces, under an eCO_2-induced nutrient limitation (H3). The effect of an increased fine root biomass on nutrient uptake was limited in our simulations and the ambient fine root allocation fractions were highly variable among the models, ranging from 5 to 30% of NPP (Supplementary Figs. 4 and 6). Both these modelled results highlight the model deficiencies in below-ground processes[37] that need addressing (Table 1). There is evidence that phosphatase activity in the litter and soil and the presence of low-molecular-weight acids used to liberate P from organic matter or from mineral surfaces increase with plant P demand[38]. This was predicted by ELM-CTC in our simulations, which also showed Amazon-wide that with "enhanced phosphatase production, productivity in the highly P-limited areas can be sustained under elevated CO_2 conditions"[39]. Plants invest in P liberation and acquisition, but whether these mechanisms can be upregulated under eCO_2 and over what time frame this may occur remain open questions. Quantification of such a response is lacking, as are estimates of the associated plant C costs to acquire P via these and other mechanisms, such as mycorrhizal symbiosis[15,40] (Table 1). The P gain and C cost for P acquisition mechanisms, as well as the associated plant–soil–microbial interactions, need to be assessed by analyses of soil, microbial and root nutrition, and via novel techniques to investigate enzyme and labile C dynamics[41]. Monitoring of below-ground fine root dynamics needs to include the surface litter layer, commonly explored by fine roots in P-impoverished ecosystems in the Amazon, but not yet quantified nor considered in ecosystem models (Table 1).

Implications of P control on the CO_2 fertilization effect

Previous model projections suggest a sustained fertilization effect of eCO_2 on the Amazon C sink, but did not consider feedbacks from a low soil P availability across much of the Amazon basin[5,6]. Our study demonstrates that, based on the current generation of CNP models, the omission of P feedbacks is highly likely to cause an overestimation of the Amazon rainforest's capacity to sequester atmospheric CO_2. Considering the P limitation on the CO_2 fertilization effect in future predictions may indicate that the forest is less resilient to higher temperatures and changing rainfall patterns than previously thought[6,42]. Periods of water deficit may contribute to the eCO_2 fertilization effect on productivity due to its water-saving effect[34], or due to alterations of the decomposition processes. Our study site experienced years with significantly less than average precipitation, for example, in 2000 and 2009; however, in our simulations this only marginally increased the positive response of GPP and NPP to eCO_2 (Supplementary Figs. 8 and 9). Models lack the appropriate sensitivity for plant responses to changes in water availability, and even more so when precipitation sums are

high[43]. Interactions of water and P availability and their consequences on the CO_2 fertilization effect remain uncertain[44] and so this is an area in which field measurements will allow us to better constrain model responses (Table 1).

Although P is likely to reduce the biomass C sink response to CO_2 in regions with a low plant-available P supply, our results suggest that plasticity in plant P use and plant P acquisition mechanisms may, at least partially, alleviate the P limitation under eCO_2 and enable the CO_2 fertilization of biomass growth. The model ensemble may be interpreted as representing a range of possible tropical plant functional strategies and growth responses to a low P availability under eCO_2. Responses are expected to be species-specific, as were plant growth responses to low P supplies in another tropical region[18]. The ecosystem-scale response to P limitation under eCO_2 thus depends on the relative contributions of the various P acquisition and P use strategies across individuals, their interactions and to what extent these processes can be upregulated under eCO_2. All these ultimately need to be described and represented in a single model framework to accurately predict the Amazon rainforest's response to future climate change.

AmazonFACE has the unique opportunity to experimentally address these key areas of uncertainty, not only by integrating the proposed measurements across the seasons and at the ecosystem scale (summary in Table 1) but also by assessing species-specific responses to eCO_2 in relation to trait expression. An Amazon-wide expression of plant functional strategies may then be inferred by applying the mechanistic interplay between trait expression and edaphic conditions. The key to predicting the future of the world's largest tropical forest under climate change and eCO_2 thus lies in obtaining experimental data on, and subsequently modelling, different plant P acquisition and use strategies and their interactions in a competing plant community.

Methods

Site description

Model simulations were conducted at the AmazonFACE experimental site in Central Amazonia (2° 35′ 39′ S, 60° 12′ 29′ W). AmazonFACE is an integrated model–experiment project that aims to assess the effects of high CO_2 concentrations on the ecology and resilience of the Amazon rainforest (https://amazonface.inpa.gov.br/). The experiment is currently being established and is situated in a terra firme forest on a plateau characterized by a highly weathered, deep, clay sediment soil (with a clay fraction of 76%), classified as a geric ferralsol[45]. The site and the surrounding area have been subjected to various long-term measurement activities[25,46,47,48,49], coordinated by the Large-Scale Biosphere–Atmosphere Program (http://lba2.inpa.gov.br/) in Amazonia, and includes the 'K34' eddy covariance flux tower[26], located approximately 2 km from the AmazonFACE site. The mean annual precipitation at K34 from January 2000 to December 2015 was 2,600 mm yr^{-1}, and the mean temperature was 26 °C.

Model descriptions

Fourteen ecosystem models with contrasting representations of ecosystem functioning and nutrient cycling were applied to the experiment (Supplementary Table 3). C cycle dynamics without nutrient cycle feedbacks are represented in the C-only models (InLand, ED2 and ELM-FATES)[50,51,52], C and N dynamics are represented in the CN models (LPJ-GUESS, O-CN, JULES, CABLE-POP(CN) and GDAY(CN))[53,54,55] and C, N and P dynamics are represented in the CNP models (ELM-ECA, ELM-CTC, CABLE, CABLE-POP, ORCHIDEE and GDAY)[19,20,21,22,23,24]. Two models were included with a respective CN and CNP version (GDAY and CABLE-POP) to assess directly the effect of considering P dynamics. The other models were treated as a non-random sample from the possible C, CN and CNP modelling assumptions. Four of the models are dynamic vegetation models: CABLE-POP considers the dynamic establishment and mortality with a fixed plant functional type composition, and LPJ-GUESS, ED2 and ELM-FATES also consider dynamic plant functional type composition. Photosynthesis is based on formulations by Farquhar et al.[56] or derivations thereof in all the models[57,58] (Supplementary Table 3).

Prognostic C allocation fractions are based on functional relationships among the tissues, for example, fixed ratios between sapwood and leaf area in CABLE-POP, LPJ-GUESS, ED2, GDAY, ORCHIDEE, O-CN, JULES and ELM-FATES, and on resource dependence, for example, higher root allocation under water or nutrient stress in LPJ-GUESS, ELM-ECA, GDAY, O-CN, ORCHIDEE, ED2 and ELM-FATES. C allocation fractions are fixed in InLand and CABLE.

Nutrient limitation is determined by the difference between demand and supply (via root uptake and resorption) of N or P, with the most limiting nutrient determining the degree of limitation. The photosynthetic parameters V_{cmax} and/or J_{max} are controlled by the leaf N in all the CN and CNP models except JULES, and leaf P additionally downregulates GPP in all the CNP models except ORCHIDEE. N controls the NPP in some of the models, namely, O-CN, JULES, ORCHIDEE, CABLE and CABLE-POP, and additionally downregulates growth efficiency (GPP/leaf area index) in CABLE and CABLE-POP.

Maintenance respiration is dependent on the temperature in all the models and is additionally controlled by the tissue N content in all the models that consider the N cycle with the exception of GDAY, in which autotrophic respiration is a fixed fraction of GPP. Plant tissue stoichiometry in the CN and CNP models is either fixed (ELM-CTC and JULES) or varies within or without bounds (all the other models). The nutrient resorption rates in the CN and CNP models are always fixed fractions of the nutrient content in leaves and roots. Competition for nutrients between plant uptake and decomposition processes is handled differently. Nutritional demands for the decomposition process (which represents microbial demands) are first met entirely in some models (CABLE, O-CN, ORCHIDEE and GDAY), are based on relative demands

between decomposition and plant uptake (ELM-CTC) or are determined via a multiple consumer approach, which includes adsorption to mineral surfaces (ELM-ECA). Nutrient uptake is a function of plant demand and nutrient availability in all the models and is further controlled by a measure of the root mass in LPJ-GUESS, GDAY, ORCHIDEE and O-CN.

Soil organic matter (SOM) decomposition is limited by soil mineral N availability in most CN and CNP models (except O-CN and ORCHIDEE) and additionally by labile P availability in most CNP models (except GDAY and ORCHIDEE). P in SOM can also be mineralized via phosphatase, decoupling the P cycle from the C and N cycle, termed biochemical P mineralization in the P models. Biochemical P mineralization is a function of the slow SOM pool turnover in CABLE, CABLE-POP and GDAY, as well as substrate availability in ORCHIDEE, ELM-ECA and ELM-CTC. Biochemical P mineralization is upregulated with higher plant P stress, representing higher phosphate production (not specified if by plants or microbes), in ELM-ECA, ELM-CTC and ORCHIDEE.

N inputs originate from N deposition (prescribed by model protocol) and N fixation (prescribed individually). N fixation is either fixed, calculated empirically as a fraction of NPP or evapotranspiration (GDAY, JULES, ORCHIDEE, ELM-CTC, LPJ-GUESS, CABLE, and CABLE-POP), or based on an optimization scheme (ELM-ECA and O-CN). P inputs originate from weathering (prescribed individually) and deposition (prescribed by model protocol). Release of P from rock weathering is a fixed, soil type-specific rate in CABLE and CABLE-POP, a function of the parent P pool in ELM-ECA, ELM-CTC, and GDAY or described as a function of lithology, runoff and air temperature in ORCHIDEE. N and P losses occur from leaching, modelled as a function of the size of the labile P and mineral N pool, respectively, and additionally controlled by runoff in ELM-ECA and ORCHIDEE.

The number of inorganic P pools and their precise definition varies among the models. We consider two inorganic P pools relevant for our analysis: the labile P pool and the secondary P pool. The labile P pool encompasses plant-available inorganic P, represented in most CNP models by two separate pools connected by sorption dynamics and effectively in equilibrium (described by Langmuir dynamics in most models and a linear approach in ORCHIDEE). The labile P pools follow different nomenclature in the models but are comparable in functionality: the P in soil solution (called labile or solution P) is readily available to plants in the model time step, whereas the non-dissolved P (referred to as sorbed or sorbed labile P pool) can become available to plants on yearly-to-decadal timescales due to desorption. The secondary P pool represents P strongly sorbed by minerals, which is largely unavailable but may enter the labile P pool on centennial timescales and, depending on the model assumptions, may be driven by plant P stress.

Model simulations

The models were forced with 16 years of observed local meteorology (2000 to 2015) from the K34 flux tower[26]. Meteorological data from July 1999 to December 2015 of near-surface air temperature, rainfall, downward shortwave radiation, downward longwave radiation, vapour pressure deficit, surface pressure, relative humidity and wind speed were available for the model input. Specific humidity was calculated based on the observed relative humidity and surface pressure. All the data time series were subject to quality control (that is, removal of outliers) and gap filling using the variables' climatological mean. Precipitation data gaps were filled from a nearby weather station of the Tropical Rainfall Measuring Mission network.

Simulations were initialized with a spin-up routine that resulted in equilibrium conditions of C stocks (and N and P, if applicable) that represented the year 1850. The 16-year meteorological time series were continuously repeated throughout the whole spin-up, during the transient phase (1851–1998) and during our model–experiment phase (1999–2013), representative of a 15-year long AmazonFACE experiment. Global data sets were used as the inputs for atmospheric CO_2 (refs [59,60]), N deposition[61,62] and P deposition[63]. Atmospheric CO_2, N and P deposition levels were set to 284.7 ppm, 1.43 kg N ha^{-1} yr^{-1} and 0.144 kg P ha^{-1} yr^{-1}, respectively, in 1850 and followed historical changes during the transient and model experiment phase.

Other site parameters used for the parameterization of the models were derived from in situ measurements and include rooting and soil depth (set to rooting depth), soil hydraulic parameters, specific leaf area and soil texture (Supplementary Table 2). Soil hydraulic parameters were derived from pedotransfer functions[64] and site-specific measurements of the soil properties[65]. Soil hydraulic parameters were included in models that accounted for this functionality to allow for a better representation of the soil water dynamics in tropical soils (Supplementary Table 2).

Two model experiments were performed over the 15-year long experiment phase by each model to assess the effect of elevated CO_2: (1) the ambient run and (2) the elevated CO_2 run. In the ambient run, the atmospheric CO_2 was set to ambient levels and employed for the model evaluation against in situ measurements, which included C fluxes from the K34 flux tower. The elevated CO_2 run represents the planned AmazonFACE experiment with a step change increase of 200 ppm at the start of the model experiment and continuous tracking of the CO_2 levels in the ambient run plus 200 ppm thereafter. Model outputs were analysed in biological years of seasonality (July to June) and the differences between the elevated CO_2 runs and the control runs were used to infer the model-based CO_2 effect.

Model output analysis

The analysis of the modelled output includes an evaluation of the modelled ambient conditions relative to in situ observations and hypotheses-based analyses of the modelled CO_2 responses. We employed a structural analysis of the model simulations[9,66,67,68] by splitting the model outcomes into the

underlying processes to identify crucial model assumptions that determine the diverging predictions for the FACE experiment. We focus here on the simulated increase in biomass C due to eCO_2 and the underlying nutrient control thereon.

Biomass C dynamics are a result of primary productivity, C allocation and turnover. We first analysed the effect of eCO_2 on GPP, NPP, autotrophic respiration and the resulting plant CUE. We then assessed changes in the NPP allocation fractions to the biomass compartments of wood, fine roots and leaves, and the resulting effect on biomass C turnover in response to eCO_2. Specific tissue turnover rates were fixed in all the models, but the overall biomass C turnover changes as a result of changing the C allocation to tissue compartments. The turnover rates of biomass C pools were calculated as the fraction of the total litter fall per total biomass pool size (Supplementary Table 4).

Plant nutrient cycle feedbacks to eCO_2 were assessed by splitting the responses into plant N uptake and plant N use efficiency and similarly into plant P uptake and PUE. The responses of N use efficiency and PUE to eCO_2 were further split into changes in tissue C allocation (differing in C:N and N:P ratios) and changes in tissue stoichiometry (flexible C:N and N:P ratios). The soil nutrient cycle feedbacks to eCO_2 were determined by separating eCO_2 responses in the N and P mineralization rates (N and P mineralization from the microbial decomposition of SOM and the biochemical P mineralization of organic P via phosphatase) and the balance of the ecosystem N and P inputs (N fixation, N and P deposition, and P weathering) and losses (N and P leaching).

Data availability

Model output data used for the analyses and figures are archived in a GitHub repository (https://github.com/Kaaze7/AmzFACE-model-ensemble-2019).

Code availability

Code used for the analyses and figures are archived in a GitHub repository (https://github.com/Kaaze7/AmzFACE-model-ensemble-2019).

References

1. Brienen, R. J. W. et al. Long-term decline of the Amazon carbon sink. Nature 519, 344–348 (2015).

2. Phillips, O. L. & Brienen, R. J. W. Carbon uptake by mature Amazon forests has mitigated Amazon nations' carbon emissions. Carbon Balance Manag. 12, 1 (2017).

3. Cernusak, L. A. et al. Tropical forest responses to increasing atmospheric CO2: current knowledge and opportunities for future research. Funct. Plant Biol. 40, 531–551 (2013).

4. Ciais, P. et al. in Climate Change 2013: Te Physical Science Basis (eds Stocker, T. F. et al.) 465–570 (Cambridge Univ. Press, 2013).

5. Cox, P. M. et al. Sensitivity of tropical carbon to climate change constrained by carbon dioxide variability. Nature 494, 341–344 (2013).

6. Huntingford, C. et al. Simulated resilience of tropical rainforests to CO_2-induced climate change. Nat. Geosci. 6, 268–273 (2013).

7. Talhelm, A. F. et al. Elevated carbon dioxide and ozone alter productivity and ecosystem carbon content in northern temperate forests. Glob. Chang. Biol. 20, 2492–2504 (2014).

8. Norby, R. J., Warren, J. M., Iversen, C. M., Medlyn, B. E. & McMurtrie, R. E. CO_2 enhancement of forest productivity constrained by limited nitrogen availability. Proc. Natl Acad. Sci. USA 107, 19368–19373 (2010).

9. Zaehle, S. et al. Evaluation of 11 terrestrial carbon–nitrogen cycle models against observations from two temperate Free-Air CO_2 Enrichment studies. New Phytol. 202, 803–822 (2014).

10. Hofansl, F. et al. Amazon forest ecosystem responses to elevated atmospheric CO_2 and alterations in nutrient availability: flling the gaps with modelexperiment integration. Front. Earth Sci. 4, 19 (2016).

11. Norby, R. J. et al. Model-data synthesis for the next generation of forest Free-Air CO_2 Enrichment (FACE) experiments. New Phytol. 209, 17–28 (2016).

12. Lloyd, J., Bird, M. I., Veenendaal, E. M. & Kruijt, B. in Global Biogeochemical Cycles in the Climate System 95 (eds Schulze, E.-D. et al.) 95–114 (Academic, 2001).

13. Vitousek, P. M. Litterfall, nutrient cycling, and nutrient limitation in tropical forests. Ecology 65, 285–298 (1984).

14. Quesada, C. A. et al. Basin-wide variations in Amazon forest structure and function are mediated by both soils and climate. Biogeosciences 9, 2203–2246 (2012).

15. Lambers, H., Raven, J. A., Shaver, G. R. & Smith, S. E. Plant nutrientacquisition strategies change with soil age. Trends Ecol. Evol. 23, 95–103 (2008).

16. Reed, S. C., Yang, X. & Tornton, P. E. Incorporating phosphorus cycling into global modeling eforts: a worthwhile, tractable endeavor. New Phytol. 208, 324–329 (2015).

17. Jiang, M., Caldararu, S., Zaehle, S., Ellsworth, D. S. & Medlyn, B. E. Towards a more physiological representation of vegetation phosphorus processes in land surface models. New Phytol. 222, 1223–1229 (2019).

18. Turner, B. L., Brenes-Arguedas, T. & Condit, R. Pervasive phosphorus limitation of tree species but not communities in tropical forests. Nature 555, 367–370 (2018).

19. Goll, D. S. et al. A representation of the phosphorus cycle for ORCHIDEE (revision 4520). Geosci. Model Dev. 10, 3745–3770 (2017).

20. Wang, Y.-P., Law, R. M. & Pak, B. A global model of carbon, nitrogen and phosphorus cycles for the terrestrial biosphere. Biogeosciences 7, 2261–2282 (2010).

21. Haverd, V. et al. A new version of the CABLE land surface model (Subversion revision r4601) incorporating land use and land cover change, woody vegetation demography, and a novel optimisation-based approach to plant coordination of photosynthesis. Geosci. Model Dev. 11, 2995–3026 (2018).

22. Comins, H. N. & McMurtrie, R. E. Long-term response of nutrient-limited forests to CO2 enrichment; equilibrium behavior of plant–soil models. Ecol. Appl. 3, 666–681 (1993).

23. Zhu, Q., Riley, W. J., Tang, J. & Koven, C. D. Multiple soil nutrient competition between plants, microbes, and mineral surfaces: model development, parameterization, and example applications in several tropical forests. Biogeosciences 13, 341–363 (2016).

24. Yang, X., Tornton, P. E., Ricciuto, D. M. & Post, W. M. Te role of phosphorus dynamics in tropical forests—a modeling study using CLM-CNP. Biogeosciences 11, 1667–1681 (2014).

25. Malhi, Y. et al. Comprehensive assessment of carbon productivity, allocation and storage in three Amazonian forests. Glob. Chang. Biol. 15, 1255–1274 (2009).

26. Araújo, A. C. et al. Comparative measurements of carbon dioxide fuxes from two nearby towers in a central Amazonian rainforest: the Manaus LBA site. J. Geophys. Res. 107, 8090 (2002).

27. Quesada, C. A. et al. Soils of Amazonia with particular reference to the RAINFOR sites. Biogeosciences 8, 1415–1440 (2011).

28. Friend, A. D. et al. Carbon residence time dominates uncertainty in terrestrial vegetation responses to future climate and atmospheric CO2. Proc. Natl Acad. Sci. USA 111, 3280–3285 (2014).

29. Walker, A. P. et al. Predicting long-term carbon sequestration in response to CO2 enrichment: how and why do current ecosystem models difer? Glob. Biogeochem. Cycles 29, 476–495 (2015).

30. Vitousek, P. M. Nutrient Cycling and Limitation: Hawai'i as a Model System (Princeton Univ. Press, 2004).

31. Nardoto, G. B. et al. Basin-wide variations in Amazon forest nitrogen-cycling characteristics as inferred from plant and soil 15N:14N measurements. Plant Ecol. Divers. 7, 173–187 (2014).

32. Fyllas, N. M. et al. Basin-wide variations in foliar properties of Amazonian forest: phylogeny, soils and climate. Biogeosciences 6, 2677–2708 (2009).

33. Wieder, W. R., Cleveland, C. C., Smith, W. K. & Todd-Brown, K. Future productivity and carbon storage limited by terrestrial nutrient availability. Nat. Geosci. 8, 441–444 (2015).

34. Medlyn, B. E. et al. Using models to guide feld experiments: a priori predictions for the CO2 response of a nutrient- and water-limited native eucalypt woodland. Glob. Chang. Biol. 22, 2834–2851 (2016).

35. Ellsworth, D. S. et al. Elevated CO2 does not increase eucalypt forest productivity on a low-phosphorus soil. Nat. Clim. Chang. 7, 279–282 (2017).

36. Wright, S. J. et al. Plant responses to fertilization experiments in lowland, species-rich, tropical forests. Ecology 99, 1129–1138 (2018).

37. Warren, J. M. et al. Root structural and functional dynamics in terrestrial biosphere models—evaluation and recommendations. New Phytol. 205, 59–78 (2015).

38. Hoosbeek, M. R. Elevated CO2 increased phosphorous loss from decomposing litter and soil organic matter at two FACE experiments with trees. Biogeochemistry 127, 89–97 (2016).

39. Yang, X., Tornton, P. E., Ricciuto, D. M. & Hofman, F. M. Phosphorus feedbacks constraining tropical ecosystem responses to changes in atmospheric CO2 and climate. Geophys. Res. Lett. 43, 7205–7214 (2016).

40. Vicca, S. et al. Fertile forests produce biomass more efciently. Ecol. Lett. 15, 520–526 (2012).

41. Wang, Y. & Lambers, H. Root-released organic anions in response to low phosphorus availability: recent progress, challenges and future perspectives. Plant Soil https://doi.org/10.1007/s11104-019-03972-8 (2019).

42. Gatti, L. V. et al. Drought sensitivity of Amazonian carbon balance revealed by atmospheric measurements. Nature 506, 76–80 (2014).

43. Powell, T. L. et al. Confronting model predictions of carbon fuxes with measurements of Amazon forests subjected to experimental drought. New Phytol. 200, 350–365 (2013).

44. He, M. & Dijkstra, F. A. Drought efect on plant nitrogen and phosphorus: a meta-analysis. New Phytol. 204, 924–931 (2014).

Acknowledgements